Electronic Supplementary Materials for

Efficient cleavage of aryl ether C−O linkages by Rh-Ni and Ru-Ni nanoscale catalysts operating in water

Safak Bulut,[a] Sviatlana Siankevich,[a] Antoine P. van Muyden,[a] Duncan T. L. Alexander,[b] Georgios Savoglidis,[a] Jiaguang Zhang,[c] Vassily Hatzimanikatis,[a] Ning Yan,[c] and Paul J. Dyson*[a]

[a] *Institut des Sciences et Ingénierie Chimiques, Ecole Polytechnique Fédérale de Lausanne (EPFL), 1015, Lausanne, Switzerland. E-mail: paul.dyson@epfl.ch*
[b] *Interdisciplinary Centre for Electron Microscopy (CIME), Ecole Polytechnique Fédérale de Lausanne (EPFL), 1015, Lausanne, Switzerland*
[c] *Department of Chemical and Biomolecular Engineering, National University of Singapore, 4 Engineering Drive 4, 117576, Singapore*

Table of Contents:

Experimental details 2
Powder XRD analysis 5
XPS analysis 6
Catalysts characterization by transmission electron microscopy 7
Catalytic studies for model compounds with β-*O*-4, α-*O*-4 and 4-*O*-5 linkages 10
Characterization of the catalysts by transmission electron microscopy after catalysis 14
Catalytic studies for diphenyl ether catalysed by mixtures of monometallic NCs 16
Thermodynamic calculations 17
Catalytic studies for substituted ether compounds 19
Catalytic studies using beech sawdust 20
References 22

Experimental details

Catalyst preparation

$RuCl_3.3H_2O$ and $RhCl_3$ were obtained from Johnson Matthey, $NiCl_2.6H_2O$ and $NaBH_4$ obtained from ABCR and used as received. $Ru_{100-x}Ni_x$ and $Rh_{100-x}Ni_x$ nanocatalysts (NCs) (x = 0, 20, 40, 50, 60, 65, 70, 75, 80, 85, 90, 95 and 100) were prepared via low temperature reduction using $NaBH_4$ as reducing agent, where *x* represents the molar percentage of nickel metal. Stabilization of the NCs was provided by using an ionic surfactant cetyltrimethylammonium bromide (CTAB – Alfa Aesar). In a typical preparation procedure (described for $Ru_{15}Ni_{85}$), the salts of both metals, $NiCl_2{\cdot}6H_2O$ (40.4 mg, 0.17 mmol) and $RuCl_3{\cdot}3H_2O$ (7.8 mg, 0.03 mmol) were dissolved together with CTAB (100 mg, 0.274 mmol) in water (3 mL) in a 10 mL flask. The mixture was sonicated for 15 min and then placed in an ice-bath and stirred for 30 min. Next, an aqueous solution (1.5 mL) of $NaBH_4$ (20 mg, 0.529 mmol) was added dropwise under vigorous stirring. A black suspension was obtained immediately. The content of the flask was stirred for 20 min in the ice-bath, completed to 10 mL with water (20 mM aqueous suspension) and used directly in catalytic studies.

Catalytic studies

The model substrates, benzyl phenyl ether and diphenyl ether were obtained from Merck and the substituted ethers and 1-phenoxy-2-phenylethane were prepared according to literature methods.[1] All reactions were carried out under 1 atm of hydrogen in water. Reactions were conducted in 25 mL Schlenk flasks equipped with Teflon stopcocks. In a typical procedure the Schlenk flask was charged with the appropriate nanocatalyst (9.45×10^{-3} mmol, 5 mol%, 472.5 µL from a 20 mM aqueous solution) and the reaction volume was completed with water to a total volume of 1 mL. The appropriate aromatic ether (0.189 mmol) was then added and the Schlenk flask was connected to a vacuum line/hydrogen setup and the air inside the flask was removed via vacuum-hydrogen flow 4 times. The reaction mixture was heated to 95 °C for 16 h under agitation. The resulting mixture was cooled to room temperature and diethyl ether (2 mL) and 1 M aqueous HCl (1 mL) were added and the mixture stirred for a further 30 min. The organic layer was separated and the aqueous layer was extracted with diethyl ether (1 mL). The combined organic layers were analysed by GC. Reactions were performed in triplicate with errors not exceeding ± 5%.

For the catalytic studies on beech sawdust (obtained from “Triage forestier du haut lac” in Muraz, Switzerland, moisture 5 wt%) and passed through a 4 mm analytical sieve and ball milled for 20 minutes at 30 Hz, reactions were conducted in a sealed microwave vial (10 mL) pierced with a needle inside a Parr autoclave (75 mL). In a typical procedure, the vial was charged with the appropriate catalyst (0.01 mmol based on metals) and the reaction volume was completed with water to a volume of 1 mL (in some cases 1 mL of MeOH was added, see Table S11). Sawdust (50 mg) was then added and the autoclave was purged three times with hydrogen and sealed at 50 bar. The reaction mixture was heated to 150 °C for 16 or 64 h at 800 rpm. The resulting mixture was cooled to room temperature and 1 M aqueous HCl (1 mL) was added. The mixture was filtered and washed with water (3x5 mL) and ethyl acetate (3x5 mL). The organic layer was separated and the aqueous layer was extracted with ethyl acetate (3x15 mL). The organic phase was concentrated to ~1 mL on a rotary evaporator and dodecane was added as internal standard. The organic layer was analysed by GC/MS and

quantified using the effective carbon number concept.[2] The residue was dried in an oven (80°C) overnight, then cooled to room temperature in a desiccator and weighed.

Qualitative and quantitative analysis (external standard method) of the reaction products was performed using gas chromatography (GC) analysis on a Varian Chrompack CP-3380 using N_2 as carrier gas equipped with a capillary column from Agilent (length × diameter × film: 25 m × 0.25 mm × 0.25 µm) and a FID detector. The following GC oven temperature program was used: 40 °C hold for 2 min, ramp 15 °C/min to a final temperature of 250 °C and hold at this temperature for 1 min. For the studies with sawdust the following GC oven temperature program was used: 45°C hold for 5 min, ramp 20°C/min to a final temperature of 230°C and held at this temperature for 10 min.

Catalyst characterization

Transmission electron microscopy (TEM) was carried out on a Philips/FEI CM12 operated at 120 kV acceleration voltage. Scanning transmission electron microscopy (STEM) analyses were made using a FEI Osiris operated at 200 kV acceleration voltage and a FEI Titan Themis 60-300 operated at 80 kV, applying spherical aberration correction for the electron probe. Samples were prepared by dropping the nanocatalyst containing solutions onto Cu grids with continuous carbon (TEM) or holey carbon support films with ultrathin carbon windows (STEM), and allowing the solvent to evaporate. On both STEM instruments, *Z*-contrast images were recorded using the high angle annular dark-field (HAADF) detector, and energy-dispersive X-ray spectroscopy (EDS) chemical mapping was performed using the ChemiSTEM capabilities of the instruments. EDS data were acquired and processed using Bruker Esprit software. The samples were notably beam sensitive during STEM imaging, particularly under the extended electron exposure of EDS mapping. This sensitivity primarily took the form of: a) coalescence/sintering of the NCs with each other; b) a “decomposition” of the Ni-containing membrane structures which transformed their contrast from being rather smooth to lumpy or nodular on the nanoscale (see Fig. S4). In order to mitigate such beam-induced changes, EDS maps were recorded for times only up to about 5 minutes. Later measurements were performed on the Titan Themis at a lower acceleration voltage (80 kV) than initial measurements on the Osiris (200 kV), combined with lower beam currents (maximum ~0.5 nA vs ~1 nA for Osiris measurements), which appeared to slow the structural changes. Data presented here are only from these later measurements and chosen to be as representative as possible of the structural state recorded in the initial HAADF image.

Powder XRD measurements were performed on a Bruker D8 Discover diffractometer with Cu Kα radiation at 40 kV using low background holders. The NCs were collected in a 2 mL Eppendorf tube via centrifugation and separated from the aqueous phase and washed with EtOH (3×2 mL) via centrifugation. The NCs were dried under vacuum for one day and stored under nitrogen. XPS spectra were recorded on a VG ESCALAB MKII spectrometer, using mono Al Kα X-ray source (hv = 1486.71 eV, 5mA, 15 kV). The data were calibrated from the C1s signal (285.0 eV).

Inductively coupled plasma mass spectrometry (ICP-MS) was conducted on an ICP-OES 5110 instrument (Agilent) using standard metal solutions as references for each measurement. The NC solutions were centrifuged and the water phase containing inorganic residues was separated by decantation from the NCs. The remaining NCs were digested in a microwave for 2 h prior to injection into the instrument. Results: $Rh_{15}Ni_{85}$: 13.73% Rh and 86.27% Ni. $Ru_{15}Ni_{85}$: 13.69% Ru and 86.31% Ni.

To determine the adhesion of the CTAB on the NCs, the Ni NCs were separated via centrifugation from the aqueous solution. The NCs were extensively washed with water and then with ethanol and the remaining Ni NCs were dried at room temperature under vacuum (0.1 MPa) for 2 days and stored in a glove box. For ICP analysis, the sample was digested with conc. nitric acid for 2 h, and the solution dried and redissolved in water prior to injection into the instrument. The Ni content was found to be 51.1%.

Thermodynamic calculations

Chemical structures were designed and dissolution constants in aqueous medium were calculated with the Marvin Suite 6.2.0 (ChemAxon, Hungary). The standard Gibbs free energy of formation of compounds ($\Delta_f G'^0$, Table S9) and standard Gibbs free energy of reactions ($\Delta_r G'^0$, Fig. S9) were calculated using the Group Contribution Method.[3] The standard Gibbs free energy of reaction was calculated from the standard Gibbs free energy of formation of participating compounds using the equation:

$$\Delta_r G'^0 = \sum_i v_i \Delta_f G'^0_{P,i} - \sum_j v_j \Delta_f G'^0_{S,j}$$

where v_j and v_i are the stoichiometric coefficients of the participating reactants S_j and products P_i respectively.

Solution thermodynamics were used in standard conditions of temperature and pressure in order to calculate the thermodynamic parameters of compounds and reactions. These assumptions match the catalytic conditions employed here. It is assumed that the temperature is regulated and constant throughout the experiment and that the presence of hydrogen in the gas and aqueous phase is in equilibrium

Powder XRD analysis

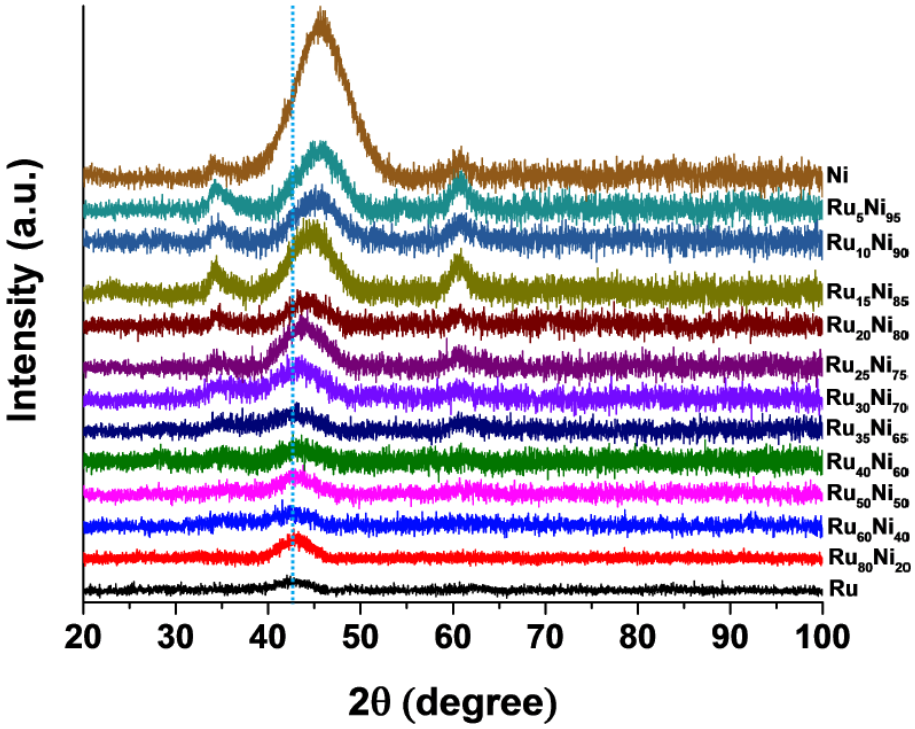

Fig. S1 XRD patterns of the $Ru_{100-x}Ni_x$ NCs. Blue dotted line shows the peak position of Ru NCs.

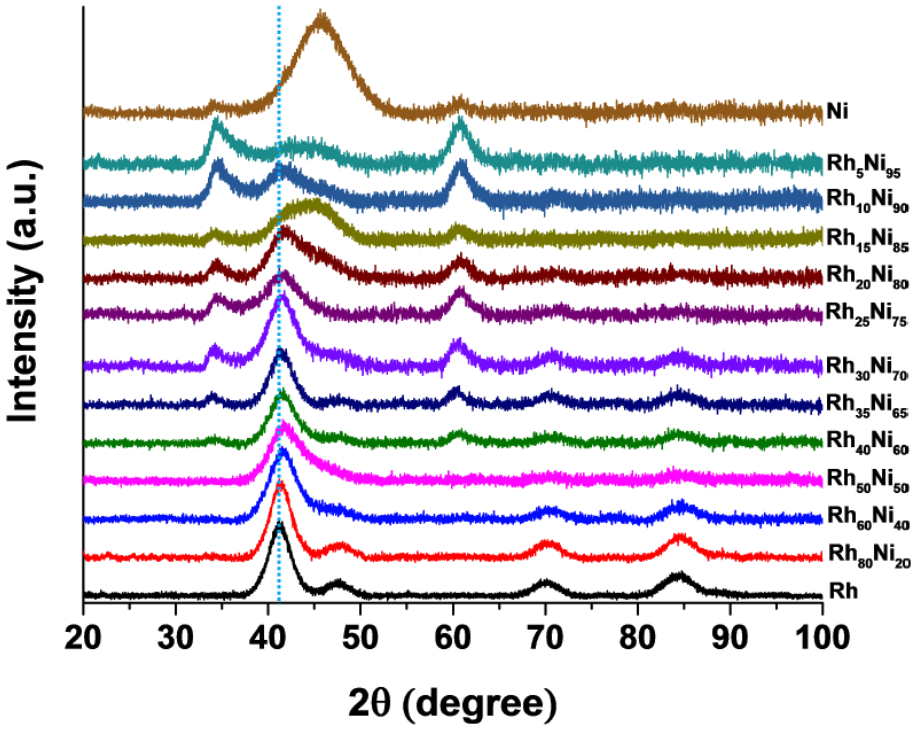

Fig. S2 XRD patterns of the $Rh_{100-x}Ni_x$ NCs. Blue dotted line shows the peak position of Rh NCs.

XPS analysis

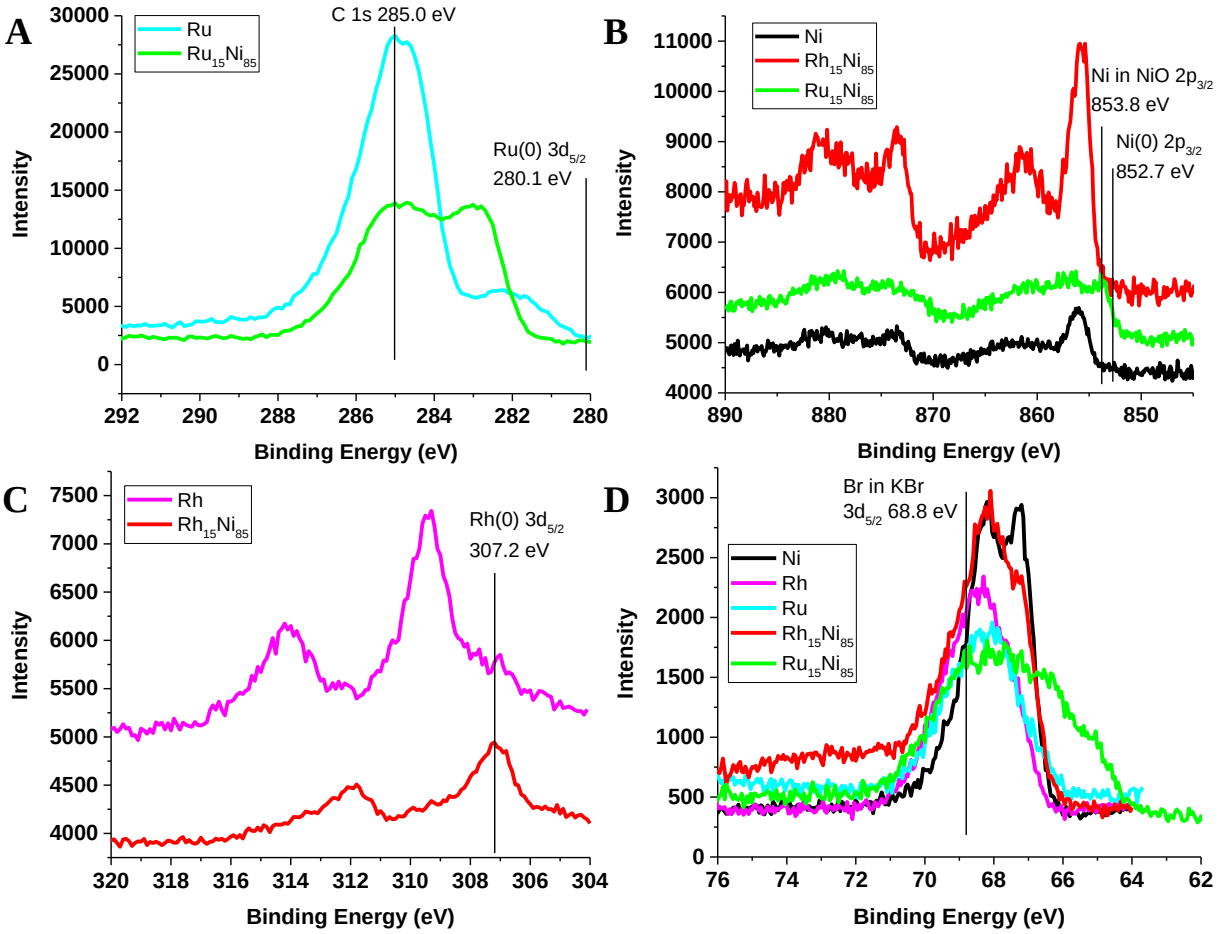

Fig. S3 XPS spectra of the $Ru_{15}Ni_{85}$, $Rh_{15}Ni_{85}$, Ru, Rh and Ni NCs. (A) Ru 3d spectra (overlapped with C 1s spectra), (B) Ni 2p spectra, (C) Rh 3d spectra and (D) Br 3d spectra.

Catalysts characterization by transmission electron microscopy

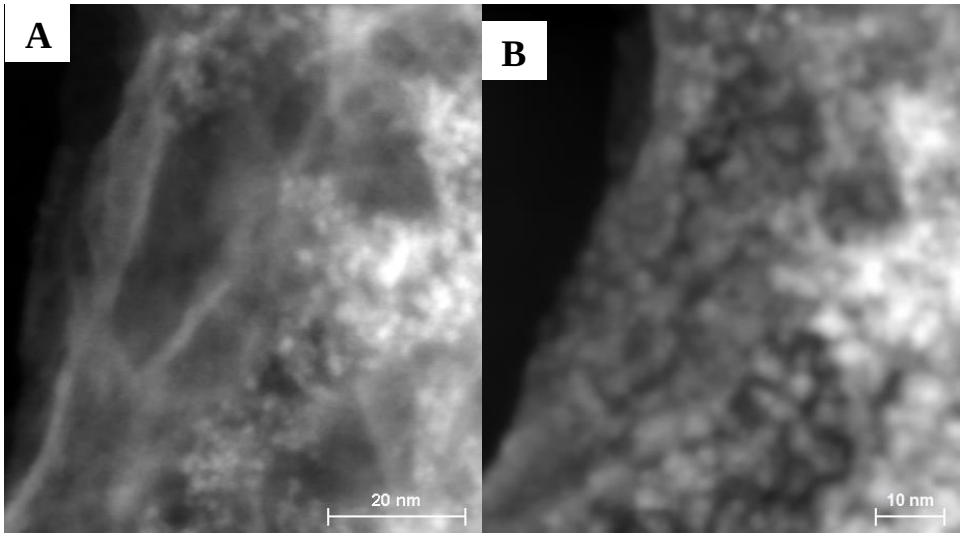

Fig. S4 Structural changes observed during STEM-EDS mapping. HAADF STEM image of a region of interest of a $Ru_{15}Ni_{85}$ sample (A) before EDS map acquisition and (B) HAADF STEM image of the same region after about 5 minutes of EDS mapping. The membrane has taken on a nodular appearance, and some sintering of the NCs appears to have occurred. Images acquired using the FEI Titan Themis at 80 kV and with 0.5 nA beam current.

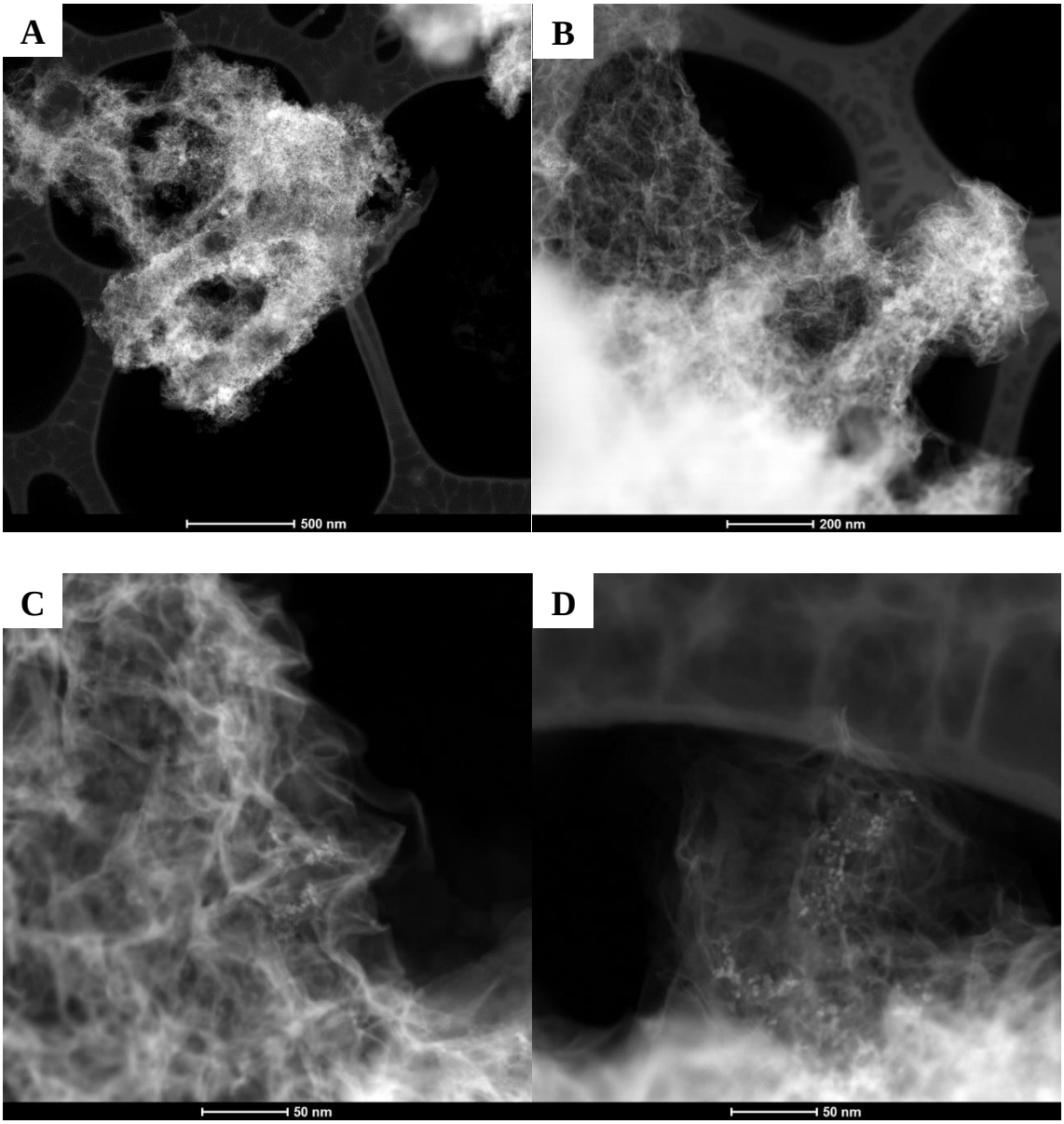

Fig. S5 Lower magnification HAADF STEM images of the $Ru_{15}Ni_{85}$ and $Rh_{15}Ni_{85}$ samples. (A) $Ru_{15}Ni_{85}$ and (B) $Rh_{15}Ni_{85}$ deposited on holey carbon support films with ultrathin carbon windows. The images demonstrate the large aggregates of the thin membranes. Embedded within the membranes are the NCs. Not all of the aggregate volumes are in focus because of their large out of plane size. (C and D) HAADF STEM images taken at a higher magnification of the $Rh_{15}Ni_{85}$ sample, showing in more detail the NCs dispersed on fluffy membrane-like material.

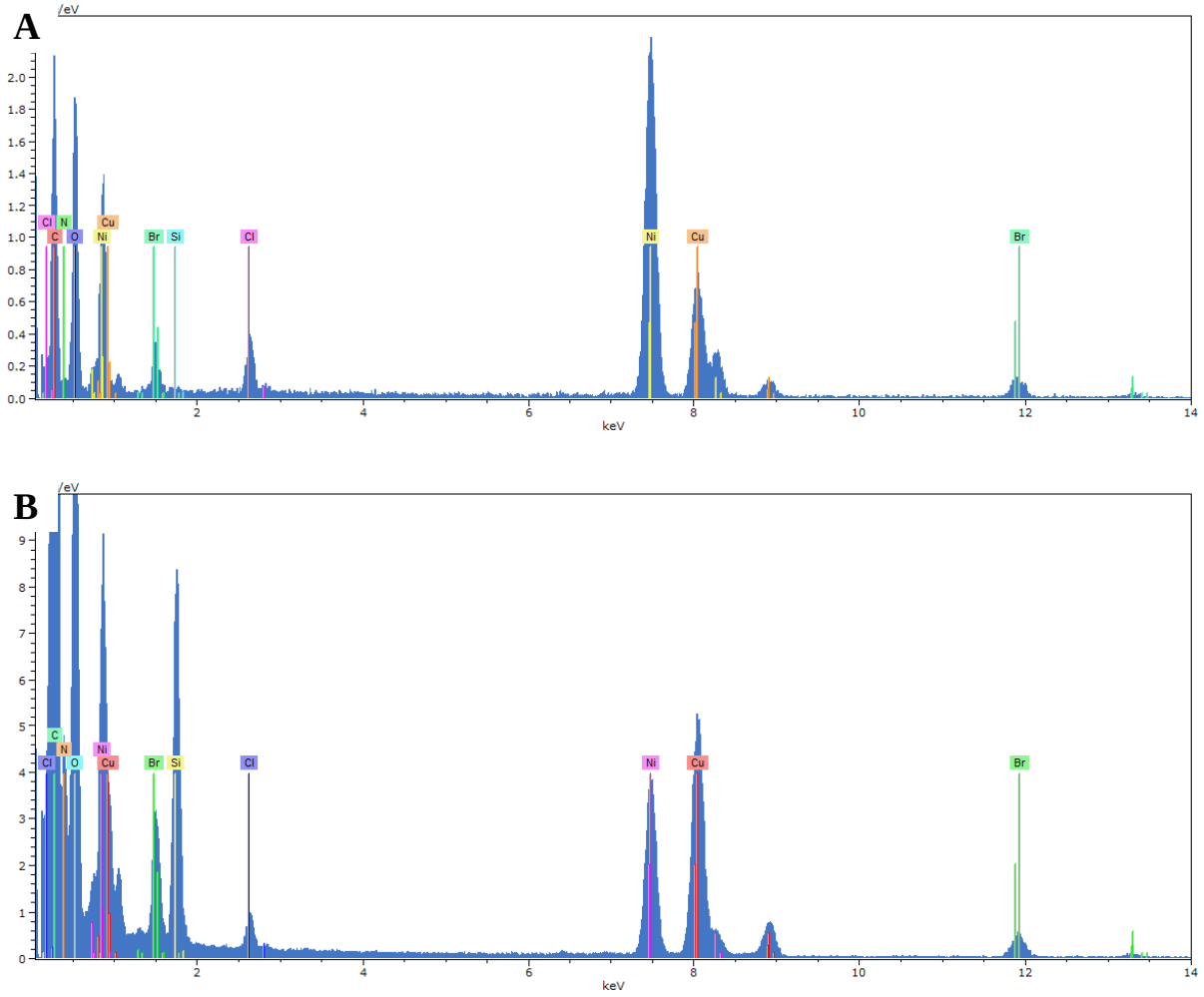

Fig. S6 EDS spectra of the membrane parts in $Rh_{15}Ni_{85}$. (A) Fresh material and (B) material taken after hydrogenolysis of diphenyl ether, integrated from regions of EDS maps which are NC free. Along with Ni, the CTAB condition includes O, Cl and Br, which are distributed uniformly with the Ni. These elements remain after reaction, with O signal increasing.

Catalytic studies for model compounds with β-*O*-4, α-*O*-4 and 4-*O*-5 linkages

Table S1 Hydrogenolysis/hydrogenation of the model compounds (α-*O*-4, β-*O*-4 and 4-O-5) using $Rh_{15}Ni_{85}$, $Ru_{15}Ni_{85}$ and Ru/C, Rh/C and Raney Ni.

Entry	Catalyst	α-*O*-4		β-*O*-4		4-O-5	
		Conv. %	Σ Dimer	Conv. %	Σ Dimer	Conv. %	Σ Dimer
1	Ru/C	43	8%	17	12%	45	5%
2	Rh/C	98	4%	89	3%	63[a]	17%[b]
3	Raney Ni	38	2%	0	2%	0	0%
4	$Rh_{15}Ni_{85}$	100	0%	97	<1%	39	<1%
5	$Ru_{15}Ni_{85}$	>99	0%	>99	<1%	57	1%

Reaction conditions: aromatic ether (0.189 mmol), catalyst (5 mol% 0.00945 mmol based on the metal), H_2O (1 mL), H_2 (1 atm), 16 h, 95 °C.
[a] Note that while the conversion of 4-O-5 model compound with the Rh/C catalyst is higher than that of the $Rh_{15}Ni_{85}$ and $Ru_{15}Ni_{85}$ catalysts, the noble metal loading in the bimetallic catalysts is considerably lower.
[b] Note that the overall yield of dimer products is lower with the bimetallic NCs.

Table S2 Hydrogenolysis/hydrogenation of 1-phenoxy-2-phenylethane (model compound for β-*O*-4 linkage) catalysed by $Ru_{100-x}Ni_x$ NCs.

Ni (%)	Yield (%)							Conv. (%)
			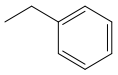	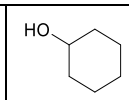	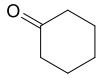	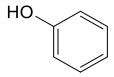	Fully hydrogenated dimer	
100	0	1	28	15	1	32	0	47
95[a,b]	2	<1	40	24	7	17	2	53
90[a,b]	1	<1	97	84	2	13	<1	>99
85[a,b]	1	<1	76	69	3	26	<1	>99
80[a,b]	1	<1	54	67	3	28	1	>99
75[a,b]	2	<1	82	71	2	22	2	>99
70[a,b,c]	1	<1	57	91	1	5	1	>99
65[a,b1,c]	2	<1	53	63	2	25	3	97
60[a,b1]	2	1	85	81	2	7	3	97
50[a1,b2,c]	2	1	91	73	2	7	4	>99
40[a,b]	2	1	35	94	2	0	1	>99
20[a1,b1,c1]	4	2	83	86	2	0	2	96
0[a1,b1,c2,d]	6	3	88	68	2	0	3	>99

Reaction conditions: 1-phenoxy-2-phenylethane (0.189 mmol), catalyst (5 mol%, 0.00945 mmol), H_2O (1 mL), H_2 (1 atm), 16 h, 95 °C. [a, a1] Ethylcyclohexane <1%,[a] 1%[a1]. [b, b1, b2] Partially hydrogenated dimer <1%,[b] 1%,[b1] 2%[b2]. [c, c1, c2] Cyclohexane <1%,[c] 1%,[c1] 2%[c2]. [d] 2-Cyclohexylethanol 2%.

Table S3 Hydrogenolysis/hydrogenation of 1-phenoxy-2-phenylethane (model compound for β-*O*-4 linkage) catalysed by $Rh_{100-x}Ni_x$ NCs.

Ni (%)	Yield (%)							Conv. (%)
	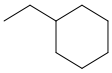	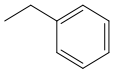	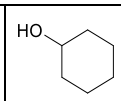	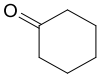	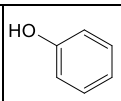	Partially hydrogenated dimer	Fully hydrogenated dimer	
100[a1]	0	28	15	1	32	0	0	47
95[a,b,c]	0	45	24	1	50	<1	<1	75
90[a,b,c]	<1	71	27	2	51	<1	<1	81
85[a,b]	0	96	27	2	59	<1	<1	97
80[a,b,c]	<1	72	42	2	50	<1	1	96
75[a,b,c]	<1	80	52	2	44	<1	1	>99
70[a1,b]	<1	97	46	2	41	<1	<1	>99
65[a,b,c]	<1	41	65	2	32	<1	<1	>99
60[a,b,c]	1	56	85	1	11	1	2	>99
50[a,b,d,e]	2	32	94	<1	<1	2	2	>99
40[a,b,c1,d]	13	47	10	40	11	20	16	98
20[a,b,d,e1,f]	22	52	70	1	<1	21	5	99
0[d1,e2,f1]	78	0	14	46	0	37	0	>99

Reaction conditions: 1-phenoxy-2-phenylethane (0.189 mmol), catalyst (5 mol%, 0.00945 mmol), H_2O (1 mL), H_2 (1 atm), 16 h, 95 °C. [a, a1] Toluene <1%,[a] 1%[a1]. [b] Benzene <1%. [c, c1] 2-Phenylethanol <1%,[c] 4%[c1]. [d, d1] Cyclohexane <1%,[d] 4%[d1]. [e, e1, e2] 2-Cyclohexylethanol 1%,[e] 2%,[e1] 9%[e2]. [f, f1] Methylcyclohexane <1%,[f] 1%[f1].

Table S4 Hydrogenolysis/hydrogenation of benzyl phenyl ether (model compound for α-*O*-4 linkage) catalysed by $Ru_{100-x}Ni_x$ NCs.

Ni (%)	Yield (%)							Conv. (%)
				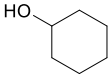	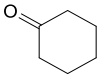	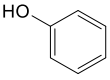	Fully hydrogenated dimer	
100	0	0	94	28	1	71	0	100
95[a]	1	0	71	0	64	34	0	98
90	1	0	98	16	0	23	0	98
85	2	0	99	3	4	45	0	>99
80	<1	0	99	12	0	27	0	>99
75	1	<1	99	31	0	11	0	>99
70	1	<1	99	33	0	2	0	>99
65	1	<1	98	27	0	19	0	98
60	1	<1	100	28	0	12	0	100
50	<1	0	97	19	3	55	0	97
40	1	<1	98	61	0	6	0	99
20[a1]	3	1	95	73	1	8	<1	99
0[a2]	5	1	85	13	3	49	<1	96

Reaction conditions: benzyl phenyl ether (0.189 mmol), catalyst (5 mol%, 0.00945 mmol), H_2O (1 mL), H_2 (1 atm), 16 h, 95 °C. [a, a1, a2] Partially hydrogenated dimer <1%,[a] 2%,[a1] 10%[a2].

Table S5 Hydrogenolysis/hydrogenation of benzyl phenyl ether (model compound for α-*O*-4 linkage) catalysed by $Rh_{100-x}Ni_x$ NCs.

Ni (%)	Yield (%)							Conv. (%)
				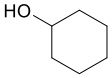	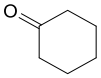	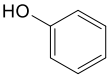	Fully hydrogenated dimer	
100	<1	0	99	9	6	82	0	>99
95	0	0	100	7	1	64	0	100
90	0	0	100	11	1	71	0	100
85	0	0	100	5	1	79	0	100
80[a]	<1	1	97	49	1	38	0	100
75	0	0	100	28	1	50	0	100
70	0	0	100	8	0	81	0	100
65	0	0	100	15	1	84	0	100
60	<1	2	98	62	<1	8	<1	>99
50[a1,b,c]	0	18	78	72	0	0	1	>99
40[b]	0	35	63	95	<1	0	2	100
20[a,b]	<1	8	92	94	0	0	0	100
0[d,b1,c1]	0	61	<1	22	36	0	32	99

Reaction conditions: benzyl phenyl ether (0.189 mmol), catalyst (5 mol%, 0.00945 mmol), H_2O (1 mL), H_2 (1 atm), 16 h, 95 °C. [a, a1] Partially hydrogenated dimer 2%,[a] <1%[a1]. [b, b1] Cyclohexane <1%,[b] 5%[b1]. [c, c1] Cyclohexylmethanol <1%,[c] 5%[c1].

Table S6 Hydrogenolysis/hydrogenation of diphenyl ether (model compound for 4-*O*-5 linkage) catalysed by $Ru_{100-x}Ni_x$ NCs.

Ni (%)	Yield (%)							Conv. (%)
			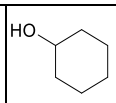	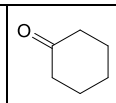	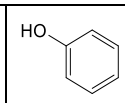	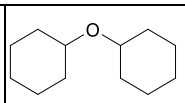	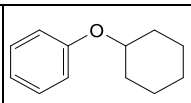	
100	5	0	3	0	2	0	<1	5
95	20	0	<1	0	4	0	<1	21
90	34	0	19	4	0	0	1	35
85	56	0	32	2	0	0	1	57
80	61	8	53	7	4	0	2	71
75	68	10	65	8	3	<1	2	81
70	76	11	68	7	2	0	2	89
65	36	7	81	2	2	0	1	86
60	50	17	76	8	4	<1	3	91
50	39	10	93	2	0	0	2	97
40	0	92	96	0	0	1	2	>99
20	42	26	94	2	0	1	3	99
0	79	9	82	3	4	0	1	90

Reaction conditions: diphenyl ether (0.189 mmol), catalyst (5 mol%, 0.00945 mmol), H_2O (1 mL), H_2 (1 atm), 16 h, 95 °C.

Table S7 Hydrogenolysis/hydrogenation of diphenyl ether (model compound for 4-*O*-5 linkage) catalysed by $Rh_{100-x}Ni_x$ NCs.

Ni (%)	Yield (%)							Conv. (%)
			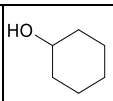	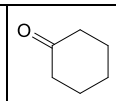	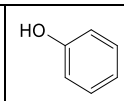	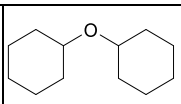	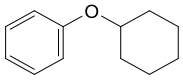	
100	5	0	3	0	2	0	<1	5
95	22	0	26	0	3	0	1	30
90	32	0	16	<1	15	0	<1	32
85	31	0	28	1	10	0	<1	39
80	26	0	31	1	13	0	2	47
75	19	0	17	<1	8	0	1	27
70	41	0	28	<1	9	0	1	42
65	15	1	32	1	7	<1	3	44
60	35	4	77	1	5	<1	4	88
50	15	47	69	7	1	8	15	>99
40	19	52	48	38	<1	6	8	>99
20	83	0	68	<1	2	1	10	93
0	0	47	67	1	0	29	0	98

Reaction conditions: diphenyl ether (0.189 mmol), catalyst (5 mol%, 0.00945 mmol), H_2O (1 mL), H_2 (1 atm), 16 h, 95 °C.

Characterization of the catalysts by transmission electron microscopy after catalysis

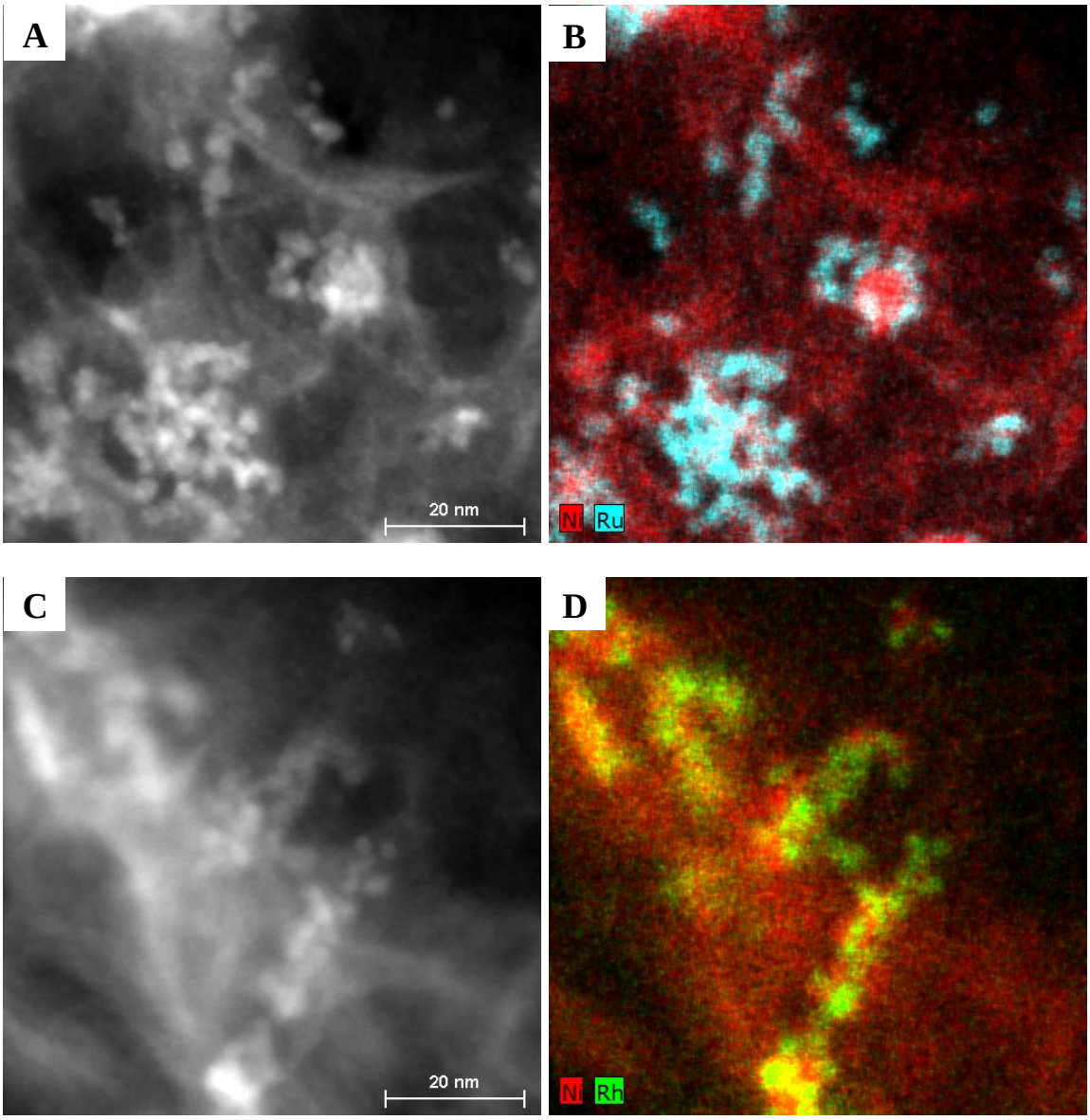

Fig. S7 Representative HAADF STEM images and corresponding EDS maps of the catalysts after reaction. (A and B) $Ru_{15}Ni_{85}$ and (C and D) $Rh_{15}Ni_{85}$ after hydrogenolysis of diphenyl ether. The morphology of NCs embedded in the membrane is preserved.

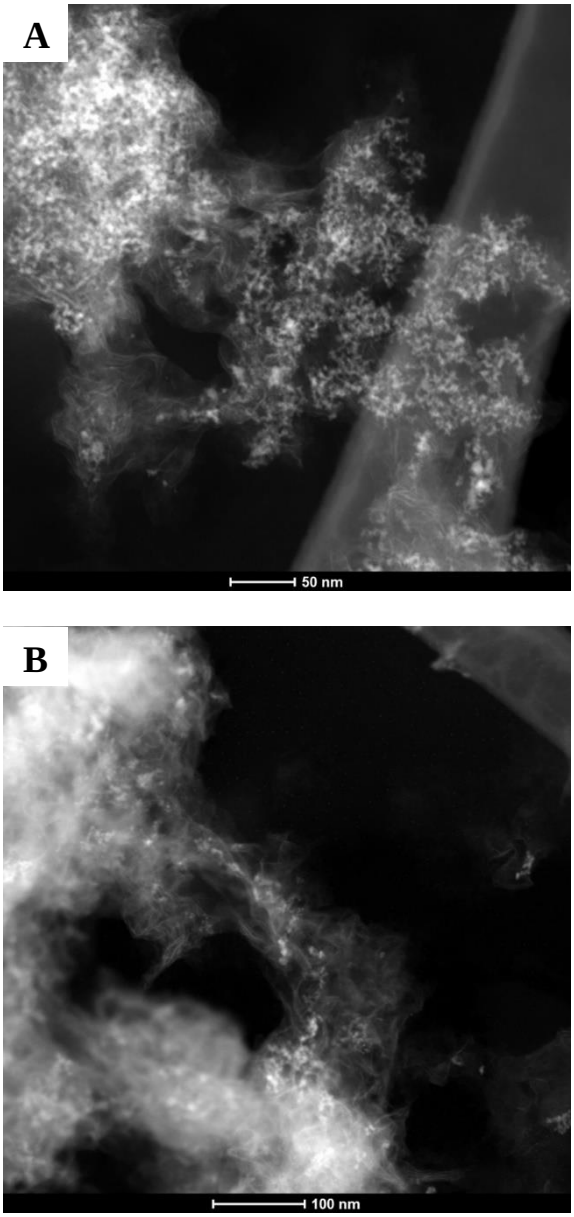

Fig. S8 HAADF STEM images of the catalysts after reaction. (A) $Ru_{15}Ni_{85}$ and (B) $Rh_{15}Ni_{85}$ after hydrogenolysis of diphenyl ether, giving a lower magnification overview than Fig. S7. The NCs are readily visible on the membranes.

Catalytic studies for diphenyl ether catalysed by mixtures of monometallic NCs

Table S8 Hydrogenolysis/hydrogenation of diphenyl ether catalysed by mixtures of monometallic NCs.

Catalyst	Yield (%)							Conv. (%)
			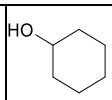	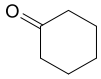	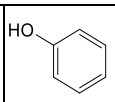	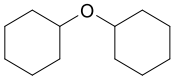	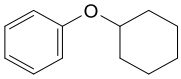	
$Ru_{15}Ni_{85}$	56	0	32	2	0	0	1	57
$Ru_{50}Ni_{50}$	39	10	93	2	0	0	2	97
15%Ru + 85%Ni	41	0	40	0	1	0	1	42
50%Ru + 50%Ni	41	0	43	0	7	0	5	55
$Rh_{15}Ni_{85}$	31	0	28	1	10	0	<1	39
$Rh_{50}Ni_{50}$	15	47	69	7	1	8	15	>99
15%Rh + 85%Ni	5	0	7	0	1	0	1	10
50%Rh + 50%Ni	21	0	19	1	4	0	2	27
$Ru_{15}Ni_{85}$ §	25	0	30	0	2	0	1	32
$Rh_{15}Ni_{85}$ §	14	0	11	0	3	0	1	15

Reaction conditions: diphenyl ether (0.189 mmol), catalyst (5 mol%, 0.00945 mmol), H_2O (1 mL), H_2 (1 atm), 16 h, 95 °C. All catalysts were prepared using CTAB as the surfactant/stabilizer unless otherwise stated. § Synthesized using cetyltrimethylammonium chloride (CTACl) as the surfactant/stabilizer.

Thermodynamic calculations

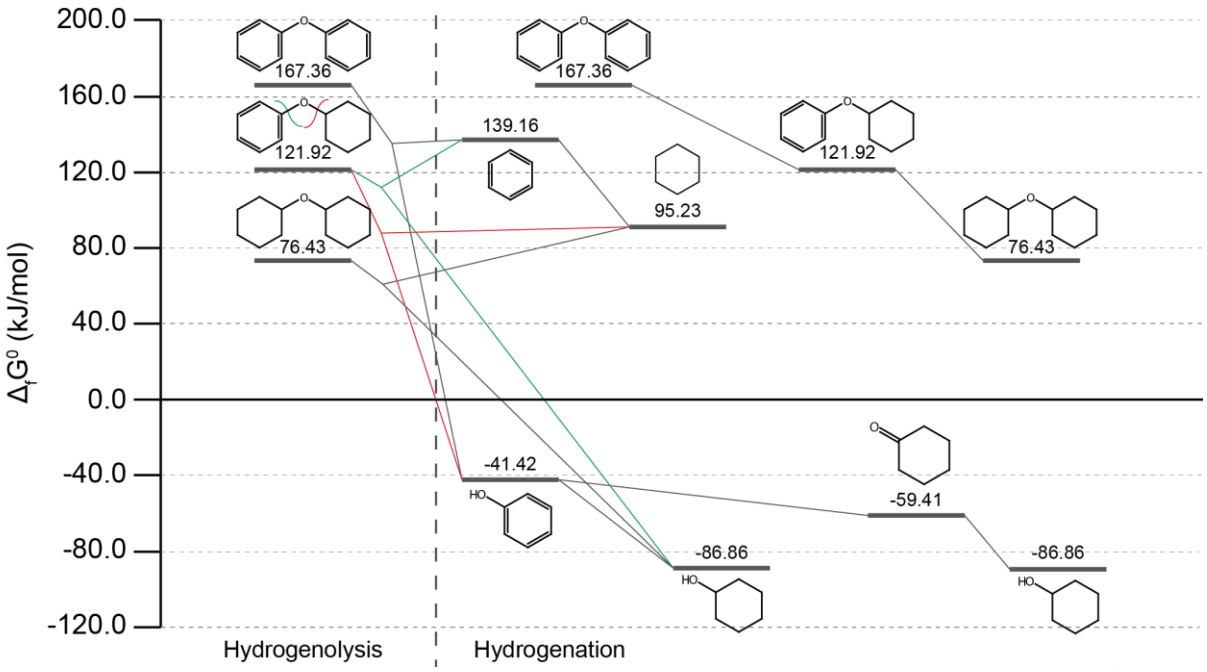

Fig. S9 Standard Gibbs free energies of formation calculated using a group contribution method for the hydrogenolysis and hydrogenation products in water.

Table S9 Standard Gibbs free energy of formation for the products obtained from diphenyl ether.

Compound	**Structure**	ΔG_f° **(KJ mol^{-1})**	ΔG_f° **error (KJ mol^{-1})**	**Formula**
Hydrogen	H-H	0	0	H_2
Diphenyl ether	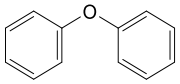	167.36	6.71	$C_{12}H_{10}O$
Benzene		139.16	5.08	C_6H_6
Phenol	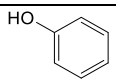	-41.42	3.29	C_6H_6O
Cyclohexanol	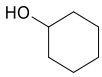	-86.86	5.27	$C_6H_{12}O$
Dicyclohexyl ether	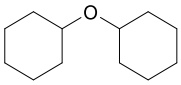	76.48	10.63	$C_{12}H_{22}O$
Cyclohexanone	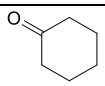	-59.41	5.31	$C_6H_{10}O$
Cyclohexyl phenyl ether	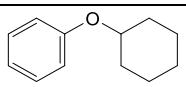	121.92	6.40	$C_{12}H_{16}O$
Cyclohexane		95.23	7.18	C_6H_{12}

Catalytic studies for substituted ether compounds

Table S10 Hydrogenolysis/hydrogenation of substituted ether compounds (related to β-*O*-4 linkage) catalysed by the $Ru_{15}Ni_{85}$ and $Rh_{15}Ni_{85}$ NCs.

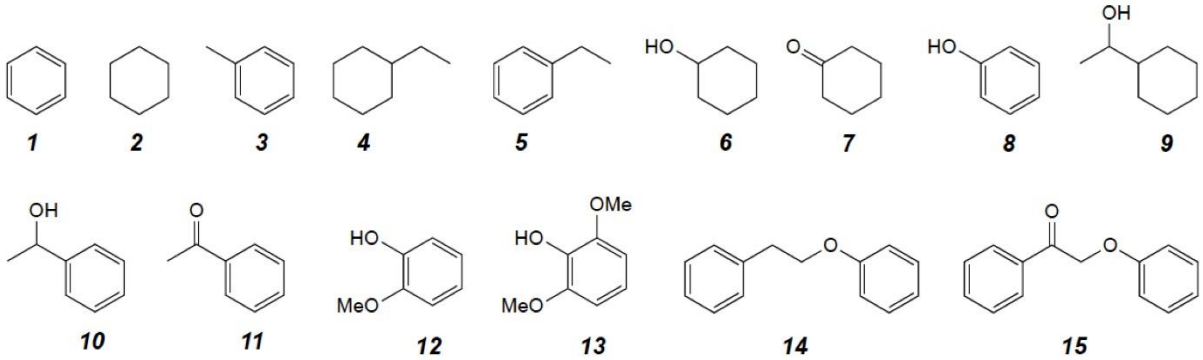

Model compound	Conversion %	Yield (%)														
		1	2	3	4	5	6	7	8	9	10	11	12	13	14	15
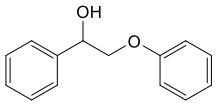	2-phenoxy-1-phenylethanol															
$Ru_{15}Ni_{85}$	>99	<1	<1	-	-	46	91	1	2	4	46	2	-	-	-	1
$Rh_{15}Ni_{85}$	>99	-	<1	1	-	12	15	3	67	<1	78	8	-	-	1	<1
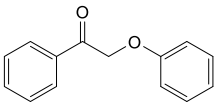	2-phenoxy-1-phenylethanone															
$Ru_{15}Ni_{85}$	>99	1	<1	-	-	34	71	1	10	3	58	4	-	-	-	1
$Rh_{15}Ni_{85}$	100	-	-	-	-	5	1	2	86	<1	88	5	-	-	1	-
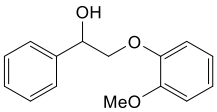	2-(2-methoxyphenoxy)-1-phenylethanol															
$Ru_{15}Ni_{85}$	100	-	-	-	<1	60	44	1	3	12	13	-	52	-	-	-
$Rh_{15}Ni_{85}$	100	-	-	<1	-	11	<1	-	1	1	88	-	82	-	-	-
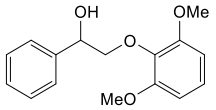	2-(2,6-dimethoxyphenyl)oxy-1-phenethanol															
$Ru_{15}Ni_{85}$	100	-	-	-	<1	58	5	-	-	22	<1	-	3	92	-	-
$Rh_{15}Ni_{85}$	100	-	-	-	-	14	-	-	-	1	81	5	-	80	-	-

Reaction conditions: aromatic ether (0.189 mmol), catalyst (5 mol%, 0.00945 mmol), H_2O (1 mL), H_2 (1 atm), 16 h, 95 °C.

Catalytic studies using beech sawdust

Table S11 Conversion of beech sawdust and yields of the four main products obtained using the $Rh_{15}Ni_{85}$ and $Ru_{15}Ni_{85}$ nanocatalysts.

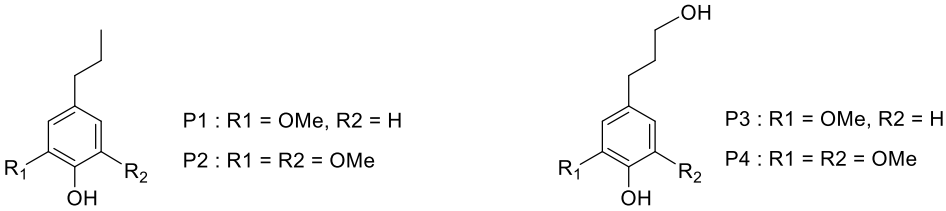

Entry	Cat.	Phenolic monomer yield [%]				Sum [%][a]	Conversion[b]
		P1	P2	P3	P4		
1		0.07	0.61	0	0	0.68	25%
2[c]	$Ru_{15}Ni_{85}$	0.12	0.74	1.97	6.01	8.83	46%
3[d]		0.45	3.11	5.89	5.52	14.96	50%
4		0.64	2.61	2.03	4.8	10.18	45%
5[c]	$Rh_{15}Ni_{85}$	1.18	5.56	3.02	10.93	20.68	56%
6[d]		2.54	9.97	3.71	8.42	24.64	57%
7[c]	None	0	0	0	0	0	41%

Reaction conditions: Beech sawdust (50 mg), catalyst (0.01 mmol, metal basis), H_2O (1mL), H_2 (50 bar), 150 °C, 16 h.
[a] GC yield were based on the maximum theoretical amount of lignin in hardwood (24 wt%).[4]
[b] Conversions were obtained from the solid residues weighed after the reaction.
[c] Addition of MeOH (1 mL).
[d] Addition of MeOH (1 mL), 64 h.

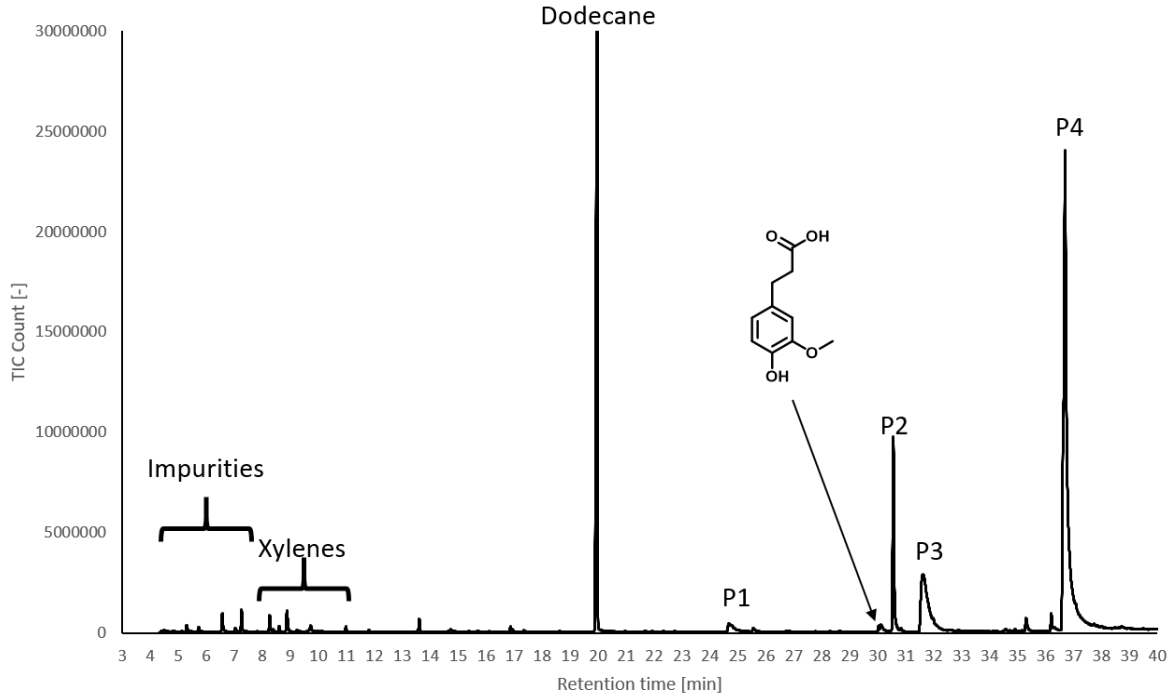

Fig. S10 GC/MS of the organic extracts after reaction corresponding to the conditions given in Table S11, entry 3.

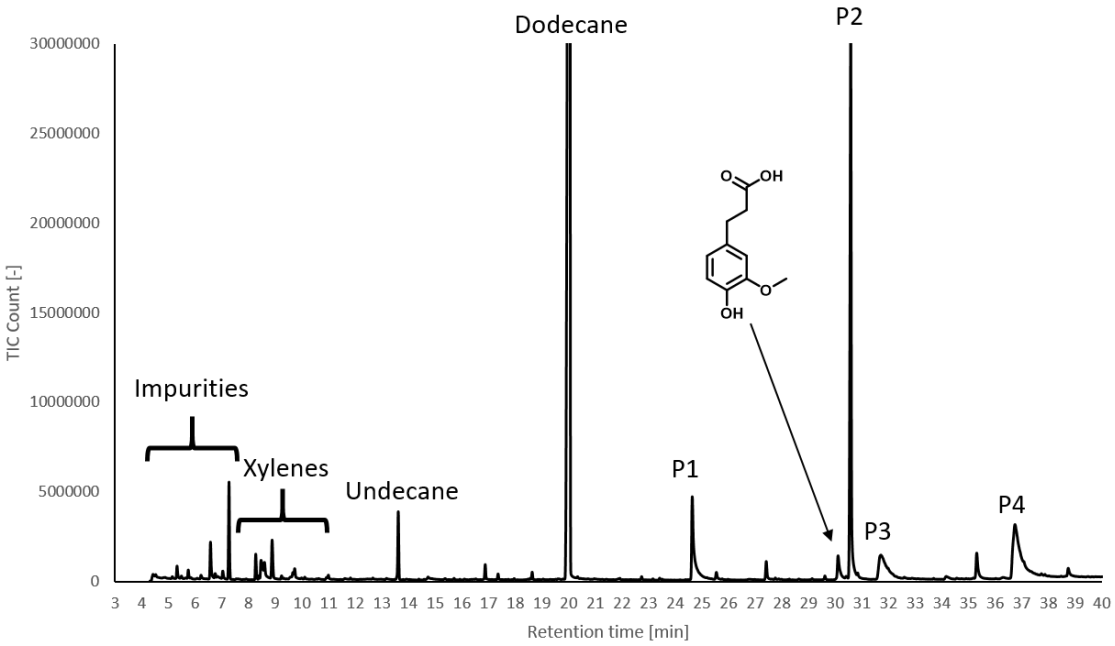

Fig. S11 GC/MS of the organic extracts after reaction corresponding to the conditions given in Table 11, entry 6.

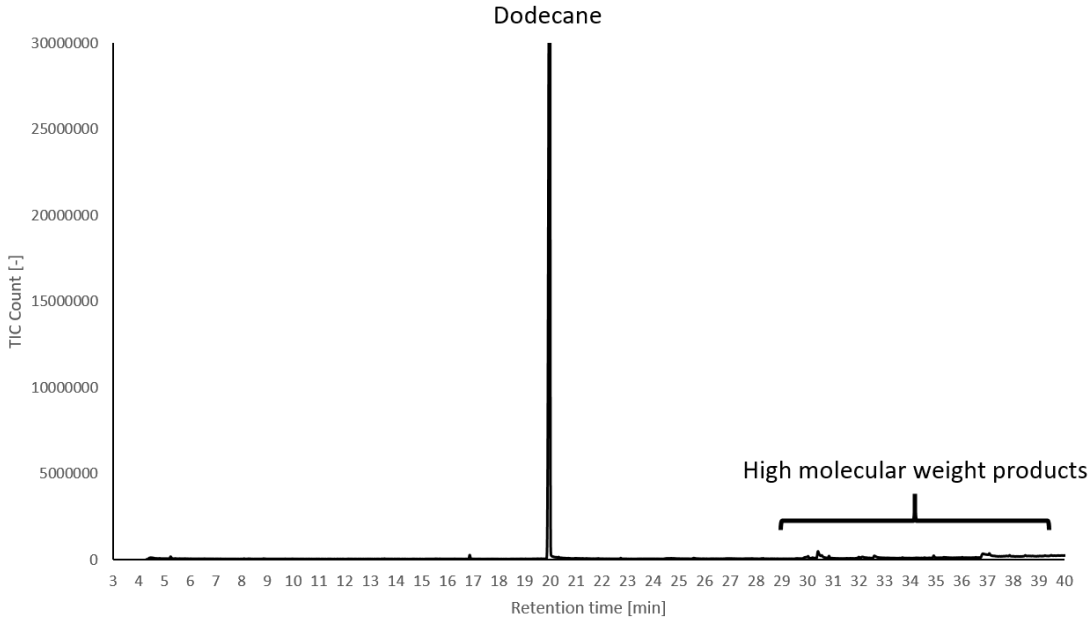

Fig. S12 GC/MS of the organic extracts after reaction corresponding to the conditions given in Table 11, entry 7.

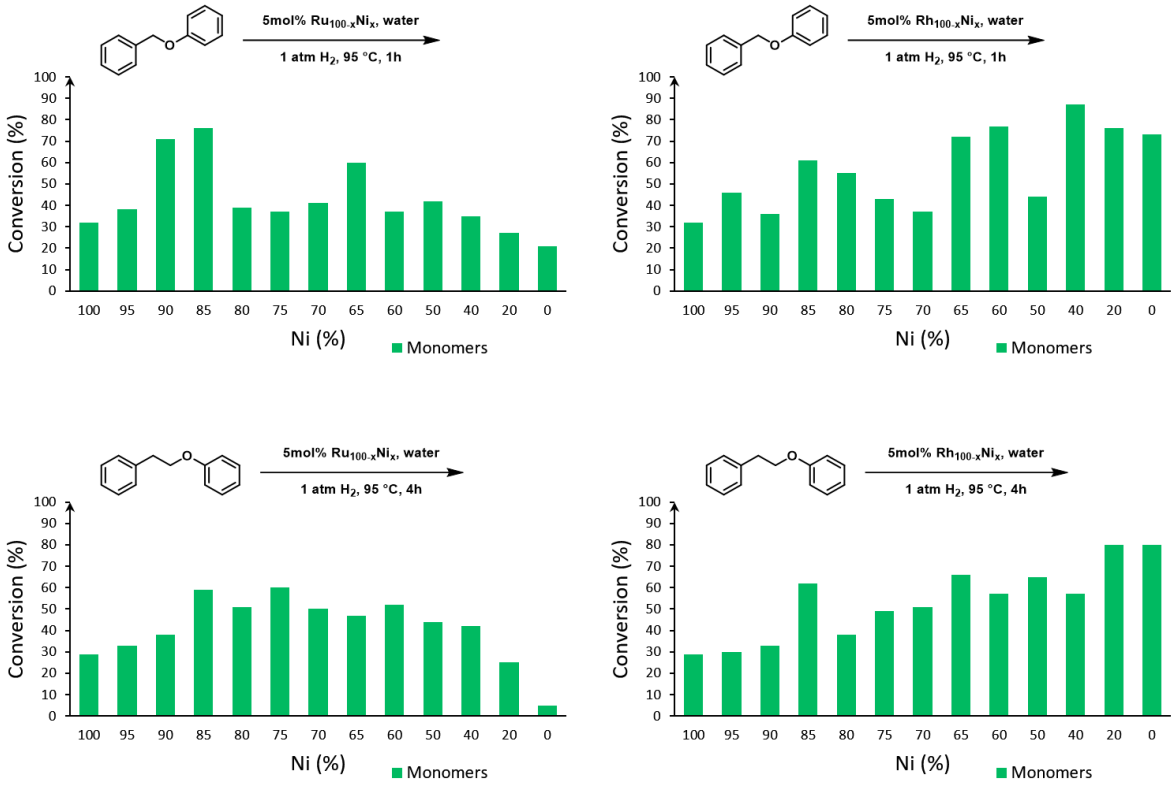

Fig. S13 Hydrogenolysis/hydrogenation of (top) benzyl phenyl ether (α-*O*-4 linkage) and (bottom) 1-phenoxy-2-phenylethane (β-*O*-4 linkage) for selected metal combinations catalyzed by (left) $Ru_{100-x}Ni_x$ NCs and (right) $Rh_{100-x}Ni_x$.

References

1 a) C. Zhao and J. A. Lercher, *Angewandte Chemie*, 2012, **124**, 6037-6042; b) M. V. Galkin, S. Sawadjoon, V. Rohde, M. Dawange and J. S. M. Samec, *ChemCatChem*, 2014, **6**, 179-184.

2 J. T. Scanlon and D. E. Willis, *Journal of Chromatographic Science*, 1985, **23**, 333-340.

3 a) M. L. Mavrovouniotis, *Journal of Biological Chemistry*, 1991, **266**, 14440-14445; b) M. L. Mavrovouniotis, *Biotechnology and Bioengineering*, 1990, **36**, 1070-1082; c) M. D. Jankowski, C. S. Henry, L. J. Broadbelt and V. Hatzimanikatis, *Biophys J*, 2008, **95**, 1487-1499.

4 V. Galkin Maxim and S. M. Samec Joseph, *ChemSusChem*, 2016, **9**, 1544-1558.